



OPEN ACCESS

EDITED BY

Yu-Chan Chang,
National Yang Ming Chiao Tung University,
Taiwan

REVIEWED BY

Imran Mohammad,
Stanford University, United States
Jieliang Zuo,
Tongji University, China

*CORRESPONDENCE

Yaodong Wang

✉ day.wang@live.cn

Weixuan Yang

✉ ywx7802@163.com

[†]These authors have contributed
equally to this work

RECEIVED 13 February 2025

ACCEPTED 05 May 2025

PUBLISHED 26 May 2025

CITATION

Shen Q, Wang S, Wu K, Wang L, Gong W,
Lu G, Chen W, Yuan C, Tu B, Li W, Wang Y
and Yang W (2025) Identification of Grb2
protein as a potential mediator of
macrophage activation in acute
pancreatitis based on bioinformatics and
experimental verification.
Front. Immunol. 16:1575880.
doi: 10.3389/fimmu.2025.1575880

COPYRIGHT

© 2025 Shen, Wang, Wu, Wang, Gong, Lu,
Chen, Yuan, Tu, Li, Wang and Yang. This is an
open-access article distributed under the terms
of the [Creative Commons Attribution License
\(CC BY\)](https://creativecommons.org/licenses/by/4.0/). The use, distribution or reproduction
in other forums is permitted, provided the
original author(s) and the copyright owner(s)
are credited and that the original publication
in this journal is cited, in accordance with
accepted academic practice. No use,
distribution or reproduction is permitted
which does not comply with these terms.

Identification of Grb2 protein as a potential mediator of macrophage activation in acute pancreatitis based on bioinformatics and experimental verification

Qinhao Shen^{1†}, Shuai Wang^{2†}, Keyan Wu^{1†}, Lihui Wang¹,
Weijuan Gong¹, Guotao Lu¹, Weiwei Chen³, Chenchen Yuan¹,
Bo Tu⁴, Wei Li⁵, Yaodong Wang^{6*} and Weixuan Yang^{2*}

¹Pancreatic Center, Department of Gastroenterology, The Affiliated Hospital of Yangzhou University, Yangzhou University, Yangzhou, China, ²Department of Gastroenterology, Huai'an Hospital Affiliated to Yangzhou University (The Fifth People's Hospital of Huai'an), Yangzhou University, Huai'an, China, ³Department of Gastroenterology, Clinical Medical College, Yangzhou University, Yangzhou, China, ⁴Clinical Research Division, Fred Hutchinson Cancer Research Center, Seattle, WA, United States, ⁵Faculty of Pharmaceutical Sciences, Toho University, Funabashi, Chiba, Japan, ⁶Department of Gastroenterology, Kunshan Hospital of Traditional Chinese Medicine, Suzhou Key Laboratory of Integrated Traditional Chinese and Western Medicine of Digestive Diseases, Kunshan Affiliated Hospital of Yangzhou University, Kunshan, China

Introduction: Macrophage activation is closely associated with Acute pancreatitis (AP). We screened and found that Growth factor receptor bound protein 2 (Grb2) is highly expressed in macrophages during AP. However, the relationship between Grb2 and AP is still poorly understood. In this study, we explored the role of Grb2 in AP.

Methods: We screened for gene affecting macrophage activation in AP by combining transcriptomics with Single-cell RNA-sequence analysis. Next, the expression of Grb2 in M1/M2 macrophage activation was detected by Single-cell RNA-sequence analysis and western blot. Furthermore, the effect of Grb2 on M1/M2 macrophage activation was detected by flow cytometry. The severity of AP was assessed by histological analysis, serum amylase, serum lipase and serum inflammatory factors *in vivo*. NOD-like receptor thermal protein domain associated protein 3 (Nlrp3) and Nuclear factor kappa-B (NF- κ B) signaling pathways were also evaluated.

Results: Grb2 is mainly expressed in macrophages of pancreas in AP and up-regulated in M1 macrophage activation. Inhibiting Grb2 could alleviate AP by preventing M1 macrophage activation through down-regulating Nlrp3 and NF- κ B.

Discussion: Inhibition of Grb2 can effectively prevent M1 macrophage activation and alleviate AP. Grb2 may potentially be an effective target of macrophage activation for the treatment of AP.

KEYWORDS

GRB2, acute pancreatitis, macrophage activation, scRNA-seq, inflammation

Introduction

AP is a prevalent gastrointestinal disease marked by acinar cell death and the infiltration of inflammatory cells (1, 2). The incidence of AP is increasing globally. Mounting evidence suggest that the infiltration of inflammatory immune cells impacts the severity of AP. The inflammatory cells infiltrated in acute pancreatitis are predominantly neutrophils and macrophages (3–6). Neutrophil forming Neutrophil Extracellular Traps (NETs) can lead to pancreatic tissue damage (7, 8). The activated macrophages in AP are mainly classified into two types. The macrophages infiltrating in the early stage of AP are generally pro-inflammatory M1 macrophage, while anti-inflammatory M2 macrophages typically play a role in the repair period of pancreatic tissue (9, 10). Hence, targeting macrophage activation could be a strategy for the treatment of AP.

Grb2 is a non-enzymatic adaptor protein consisting of a single Src homology 2 (SH2) domain and two Src homology 3 (SH3) domains (11, 12). The classic Grb2 signaling pathway is initiated by receptor tyrosine kinases (RTKs) and plays an important role in cell signal transduction. Studies have indicated that Grb2 plays a crucial role in cell proliferation (13–15), cell death (16–19) and cell differentiation (20, 21). In addition, Grb2 is closely related to immune regulation or inflammatory diseases. Treg cell-specific Grb2 deletion abrogates the augmentation of allergic airway inflammation by $Il4ra^{R576}$ (22). In the inflammatory lesions of the infected liver, Grb2 was positive in both hepatocytes and infiltrating leukocytes (23). The expression of GRB2 was increased in psoriatic lesions compared with normal skin adjacent to psoriasis and healthy controls. Inhibition of GRB2 inhibits the secretion of inflammatory mediators in keratinocytes (24). In this research, Grb2 was primarily expressed in macrophages of pancreas in AP. Inhibition of Grb2 can prevent the transformation of macrophage into M1 macrophage and alleviated pancreatic tissue injury caused by caerulein-induced AP. Thus, Grb2 may become a potential target of macrophage activation in AP.

Experimental methods

Antibodies and reagents

All reagents and antibodies involved in this study are shown in [Supplementary Tables S1, S2](#).

Animals

C57BL/6 mice were purchased from GemPharmatech Co., Ltd. (Nanjing, China). All mice were raised in a suitable environment (20–25°C, 12h light/12h dark) without specific pathogen. They were

provided with sufficient water and food. All studies were approved by Yangzhou University (No.202307018).

Construction of the AP model and Grb2 inhibitors administration

Caerulein (Cae) model, acute pancreatitis model was established by intraperitoneal (i.p.) injection of Caerulein (100 mg/kg, 1h interval, 10 times). At 0 hour, GRB2 inhibitor prexigebersen (20 mg/kg, 40 mg/kg, 80mg/kg) was administered via intravenous (i.v.) injection. 12 hours later, mice were anesthetized and euthanized. Serum samples were collected for serological analysis and ELISA assays. Pancreatic tissues were harvested and stored at -80°C for subsequent experiments.

Pancreatic duct ligation (PDL)-induced AP model: All mice were anesthetized and placed on a horizontal surgical table. A longitudinal incision of 1–2 centimeters was made on the abdomen to expose the abdominal cavity. The duodenum was turned over to expose the pancreatic duct. At a position 1 centimeter above the duodenal papilla, the tissue around the pancreatic duct was bluntly dissected, and the pancreatic duct was ligated with a ligation thread. The silk thread completely blocked it to simulate cholestasis and biliary pancreatitis caused by cholelithiasis. Then, the abdominal cavity was sutured in layers. At 1 hour, GRB2 inhibitor prexigebersen (40 mg/kg) was administered via intravenous (i.v.) injection. 24 hours later, mice were anesthetized and euthanized.

Serum samples and pancreatic tissues were harvested or subsequent experiments.

ELISA assays

Following the manufacturer's protocol, the plates were coated with antibody, sealed, and incubated overnight at 4°C. The following day, the liquid was aspirated, and the plates were washed three times with phosphate-buffered saline containing 0.05% Tween 20 (PBST). Blocking was performed using ELISPOT blocking buffer for 1 h at room temperature (RT). After removing the blocking solution and washing with PBST, serum samples and standards were added to the plates. The plates were sealed and incubated at RT for 2 h. Subsequently, the liquid was discarded, and the plates were washed three times with PBST. Detection Antibody (diluted according to the datasheet) was added, followed by sealing and incubation at RT for 1 h. After additional PBST washes, Streptavidin-HRP conjugate (1:250 dilution) was introduced, and the plates were sealed and incubated in the dark at RT for 30 min. Following further PBST washing, TMB Substrate Solution was added, and the plates were incubated in the dark at RT for 15 min. The reaction was terminated by adding Stop Solution. Absorbance was measured at 450 nm using a microplate reader.

Extraction and induction of bone marrow-derived macrophages (BMDMs)

The leg bones of the mice were isolated and soaked in 75% alcohol for 1 min. Subsequently, the bone marrow cavity was washed with 1640 medium. The cells were collected after centrifugation at 500g for 5 minutes. Macrophages were cultured in 1640 medium containing 20ng/ml macrophage-stimulating factor (M-CSF), 10% fetal bovine serum (FBS), 1% penicillin and 1% streptomycin for 7 days in 37°C, 5% CO₂ incubator. The medium was changed every other day and mature macrophages were obtained after 7 days.

Flow cytometry

Mature BMDMs were stimulated with LPS (100ng/ml) and INF γ (10ng/ml) for 24h. The BMDMs were incubated with flow cytometry antibody F4/80 (1:200 dilution) and CD86 (1:200 dilution), washed with PBS and resuspended with PBS. M1 activation of BMDM was detected by flow cytometry. Mature BMDMs were stimulated with IL-4 (50ng/ml) for 24h, incubated with flow cytometry antibody F4/80 (1:200 dilution) and CD206 (1:200 dilution) at 4°C for 30min, washed with PBS and resuspended with PBS. M2 activation of BMDM was detected by flow cytometry.

Western blot

RIPA lysis buffer and protease inhibitor (1:10) were mixed to lyse BMDMs. The BMDMs were sonicated, centrifuged at 12000 rpm at 4°C for 30 min. The protein supernatant was collected, added protein loading buffer, and boiled at 100°C for 10 min. The protein samples were subjected to SDS-PAGE, transferred to PVDF membrane. The membranes were blocked with 5% skim milk for 2 h, washed with TBST (3 times, 5 min each time), incubated with primary antibody (1:1000 dilution) overnight at 4°C. The next day, the membranes were washed with TBST (3 times, 15min each time), and incubated with second antibody (1:5000 dilution) at room temperature for 2 h. TBST washing (3 times, 10min each time). The protein bands were detected by ECL Luminometer and ImageJ was used to analyze the gray value.

Cell siRNA transfection

For one well of a 24-well plate: Diluted 2 μ L Lipofectamine 3000 (Lipo3000) in 50 μ L serum-free RPMI 1640 medium, mixed gently, and incubated at room temperature for 5 minutes. Diluted 4 μ L siRNA in 50 μ L serum-free RPMI 1640 medium, then combined this mixture with the prepared Lipo3000/1640 mixture. Mixed thoroughly and incubated at room temperature for 20 minutes to allow complex formation. Added the resulting transfection complex

mixture to the cell culture plate. After 24 hours, replaced the medium with fresh RPMI 1640 medium supplemented with 10% FBS. Performed subsequent experiments 48 hours post-transfection.

Histological analysis

Pancreatic tissue samples were fixed in 4% paraformaldehyde, paraffin-embedded, and sectioned into 5- μ m-thick slices. After deparaffinization and dehydration, the sections were stained with hematoxylin and eosin (H&E). Histopathological examination was performed using a light microscope. The severity of acute pancreatitis was evaluated according to previously established methodologies (25).

Immunofluorescence

The slices were treated with dewaxing, dehydration, membrane rupture, antigen repair, blocking. The slices were incubated with primary antibody (1:100 dilution) overnight at 4°C. On the second day, the slices were washed with PBS (3 times, 5 minutes each), incubated with secondary antibody (1:1000 dilution) at room temperature for 2 hours and washed again with PBS (3 times, 5 minutes each). Added DAPI and anti-quenching agent, then sealing. The results were detected by laser scanning confocal microscope (Nikon, Ti2-E-A1 HD25).

Isolation of Peripheral blood mononuclear cells (PBMCs)

The anticoagulated blood was layered over Ficoll separation medium, and density gradient centrifugation was performed. The PBMC layer was collected. The cells were washed with PBS, centrifuged to remove the supernatant, and lysed with lysis buffer to extract proteins.

Microarray analysis

The microarray data of AP GSE65146, GSE109227 were downloaded from Gene Expression Omnibus (GEO) database (26). Both data had been log₂ transformed. Limma package (27) was employed for identifying differentially expressed genes (DEGs). All genes ($|\log_2\text{FoldChange}| > 0$) were analyzed by Gene Set Enrichment Analysis (GSEA) via clusterProfiler package (28, 29).

RNA-seq analysis

The RNA-seq data of macrophage GSE138134 (9) and RNA-seq data of M1 macrophage activation GSE247106 (30) were downloaded from GEO database. The DEGs ($\log_2\text{FoldChange} > 0.5$, $\text{padj} < 0.01$)

were analyzed by DESeq2 package (31) or edgeR package (32–34). The pheatmap package was employed to display DEGs.

Single-cell RNA-sequence analysis

The scRNA-seq data of AP GSE188819 (35) and scRNA-seq data of macrophage activation GSE117176 (36), GSE158094 (37) were downloaded from GEO database. Downstream analysis was performed using Seurat package (V5) (38).

GSE188819: Following quality control (QC), cells with fewer than 200 expressed genes and >10% mitochondria-related genes were excluded. Harmony R package (39) was used to eliminate batch effects between different samples. As a result, a SeuratObject with 31080 cells and 22508 genes was subsequently normalized and scaled for the subsequent analysis, including RunPCA and RunTSNE. The cells were then clustered using the FindNeighbors and FindClusters functions with a resolution of 0.4. The generated clusters were visualized using T-distributed stochastic neighbor embedding (tSNE) plot.

GSE117176: Following quality control (QC), cells with fewer than 200 expressed genes and >10% mitochondria-related genes were excluded. Merge different samples. As a result, a SeuratObject with 17661 cells and 15217 genes was subsequently normalized and scaled for the subsequent analysis, including RunPCA and RunTSNE. The cells were then clustered using the FindNeighbors and FindClusters functions with a resolution of 0.1. The generated clusters were visualized using T-distributed stochastic neighbor embedding (tSNE) plot. FindMarkers was used to analyze DEGs ($\log_2\text{FoldChange} > 0.5$, $\text{padj} < 0.01$).

GSE158094: Three samples (24h_M0, 24h_M1 and 24h_M2) were selected for analysis. Following quality control (QC), cells with fewer than 200 expressed genes and >10% mitochondria-related genes were excluded. Merge different samples. As a result, a SeuratObject with 8492 cells and 12523 genes was subsequently normalized and scaled for the subsequent analysis, including RunPCA and RunTSNE. The cells were then clustered using the FindNeighbors and FindClusters functions with a resolution of 0.1. The generated clusters were visualized using T-distributed stochastic neighbor embedding (tSNE) plot. FindMarkers was used to analyze DEGs ($\log_2\text{FoldChange} > 0.5$, $\text{padj} < 0.01$).

Spearman Correlation Analysis was performed to assess the relationship between the two genes. KEGG (Kyoto Encyclopedia of Genes and Genomes) enrichment analysis were performed to analyze Genes positively associated with Grb2.

Short time-series expression miner analysis

The detection of gene clustering profiles were conducted by using the STEM (40, 41) clustering algorithm to identify temporal gene expression profiles, with the maximum number of model profiles set to 50 and maximum unit change in model profiles between time points set to 3.

Statistical analysis

Statistical analysis was performed by GraphPad Prism 8 software (GraphPad, San Diego, CA, USA) and the results were presented as mean \pm standard deviation (SD). The difference between two groups was analyzed by t-test, and the difference between more than two groups was analyzed by one-way ANOVA test. $P < 0.05$ was considered statistically significant (two-tailed).

Results

Grb2 is mainly expressed in pancreatic tissue macrophages in AP

According to the results of GSEA of pancreatic tissue microarray data of AP (GSE65146 and GSE109227), it was found that macrophage activation involved in immune response, regulation of macrophage activation, macrophage activation, positive regulation of macrophage activation were significantly up-regulated in AP (Figures 1A, B and Supplementary Table S3, S4). This indicates that macrophages in pancreas are activated when AP occurs.

We conducted a joint analysis of RNA-seq and scRNA-seq datasets (GSE117176, GSE138134, GSE158094 and GSE247106). As a result, we found a total of 184 common up-regulated DEGs. Next, a total of 3 clusters were screened by STEM clustering analysis (Supplementary Table S5). Among them, cluster 46 gene expression increased in the early stage and gradually decreased to return to the baseline level. We screened Grb2 for subsequent experiments through heatmap analysis (Figure 1C).

We obtained 24 cell clusters through cell clustering analysis on AP scRNA-seq data (GSE188819) (Figure 1D). Then we annotated different clusters based on cell-specific, highly expressed genes (Figure 1E and Supplementary Table S6). Next, we carried out cell proportion analysis. The number of macrophages increased significantly during AP (Figure 1F). FeaturePlot demonstrated that Grb2 was mainly expressed in pancreatic macrophages (Figure 1G). The results of immunofluorescence were consistent with those of scRNA-seq (Figure 1H). In addition, we detected PBMC in peripheral blood of AP patients and found that Grb2 was up-regulated in PBMC of AP patients compared with PBMC of healthy people (Supplementary Figures S1A, B). Therefore, we speculated that Grb2 may play a role in macrophage activation during AP.

Grb2 is up-regulated in M1 macrophage activation

To verify the role of Grb2 in macrophage, we initially analyzed the scRNA-seq data of macrophage activation (GSE117176) and obtained 5 cell clusters (Figure 2A). Subsequently, we performed cell annotation. M1 macrophages highly expressed Nos2, Cd86, Tnf and M2 macrophages highly expressed Chil3, Arg1, Retnla, Mgl2. M0 macrophages only expressed Ptpcr, Adgre1, Lyz2, and did not express

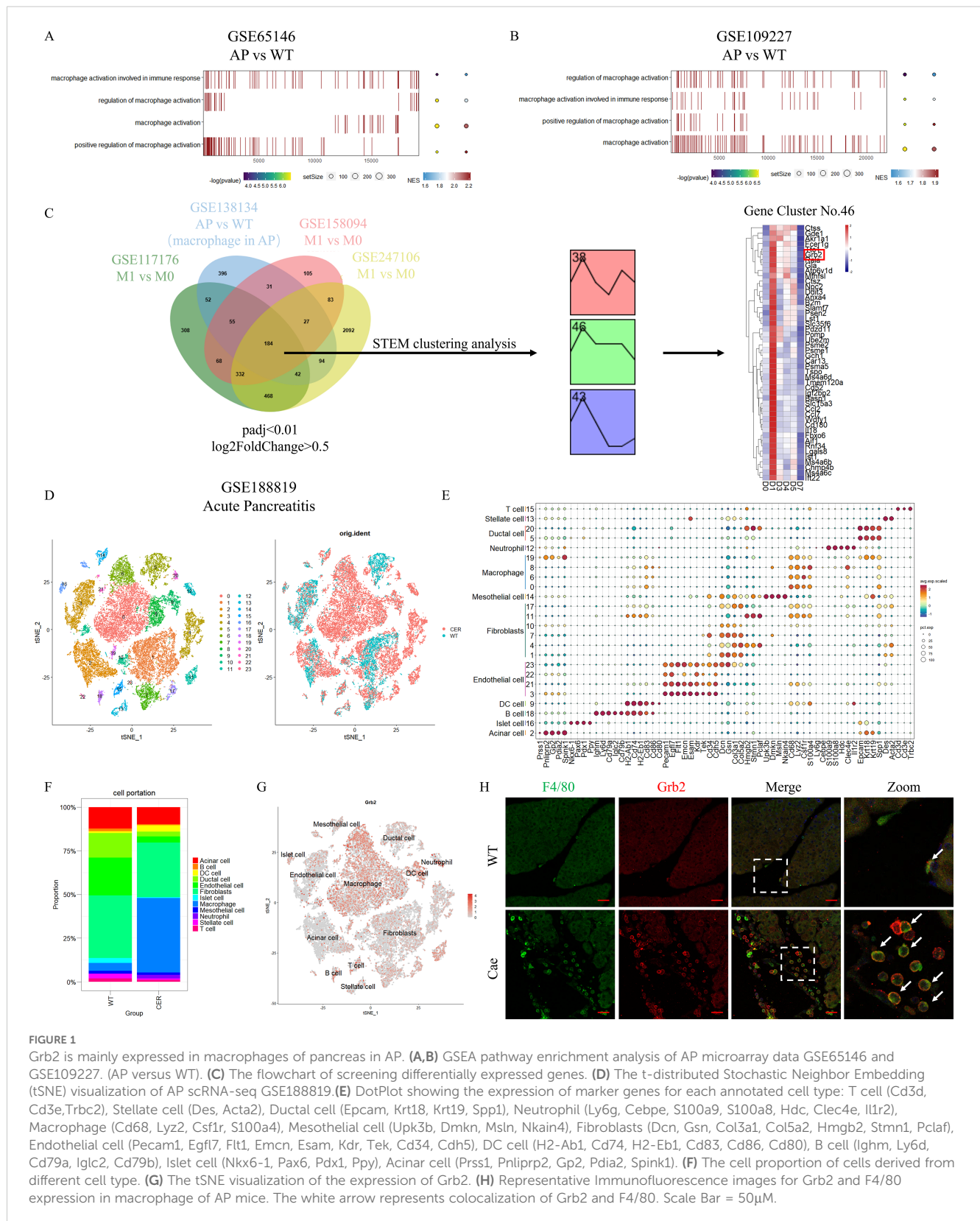
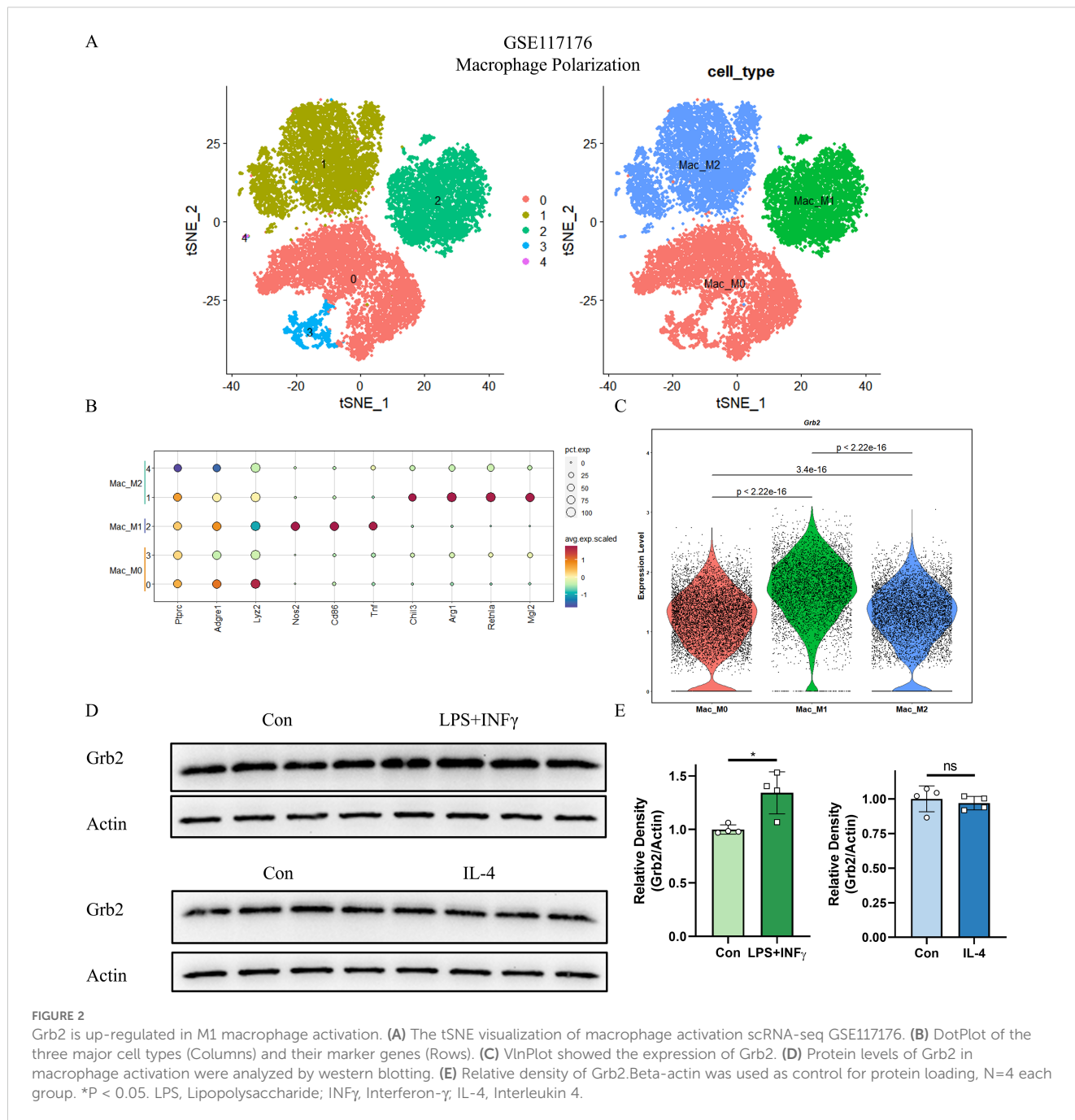


FIGURE 1

Grb2 is mainly expressed in macrophages of pancreas in AP. (A,B) GSEA pathway enrichment analysis of AP microarray data GSE65146 and GSE109227. (AP versus WT). (C) The flowchart of screening differentially expressed genes. (D) The t-distributed Stochastic Neighbor Embedding (tSNE) visualization of AP scRNA-seq GSE188819. (E) DotPlot showing the expression of marker genes for each annotated cell type: T cell (Cd3d, Cd3e, Trbc2), Stellate cell (Des, Acta2), Ductal cell (Epcam, Krt18, Krt19, Spp1), Neutrophil (Ly6g, Cebpe, S100a9, S100a8, Hdc, Clec4e, Il1r2), Macrophage (Cd68, Lyz2, Csf1r, S100a4), Mesothelial cell (Upk3b, Dmkn, Msln, Nkain4), Fibroblasts (Dcn, Gsn, Col3a1, Col5a2, Hmgb2, Stmn1, Pclaf), Endothelial cell (Pecam1, Eglf7, Ftt1, Emcn, Esam, Kdr, Tek, Cd34, Cdh5), DC cell (H2-Ab1, Cd74, H2-Eb1, Cd83, Cd86, Cd80), B cell (Ighm, Ly6d, Cd79a, Iglc2, Cd79b), Islet cell (Nkx6-1, Pax6, Pdx1, Ppy), Acinar cell (Prss1, Pnliprp2, Gp2, Pdia2, Spink1). (F) The cell proportion of cells derived from different cell type. (G) The tSNE visualization of the expression of Grb2. (H) Representative Immunofluorescence images for Grb2 and F4/80 expression in macrophage of AP mice. The white arrow represents colocalization of Grb2 and F4/80. Scale Bar = 50µM.

M1M2-specific genes. (Figure 2B). Nos2, Cd86 and Tnf were mainly expressed in M1 macrophage, while Chil3, Arg1, Retnla and Mgl2 were highly expressed in M1 macrophage (Figure 2B). The VlnPlot demonstrated that Grb2 was up-regulated in M1 macrophages and

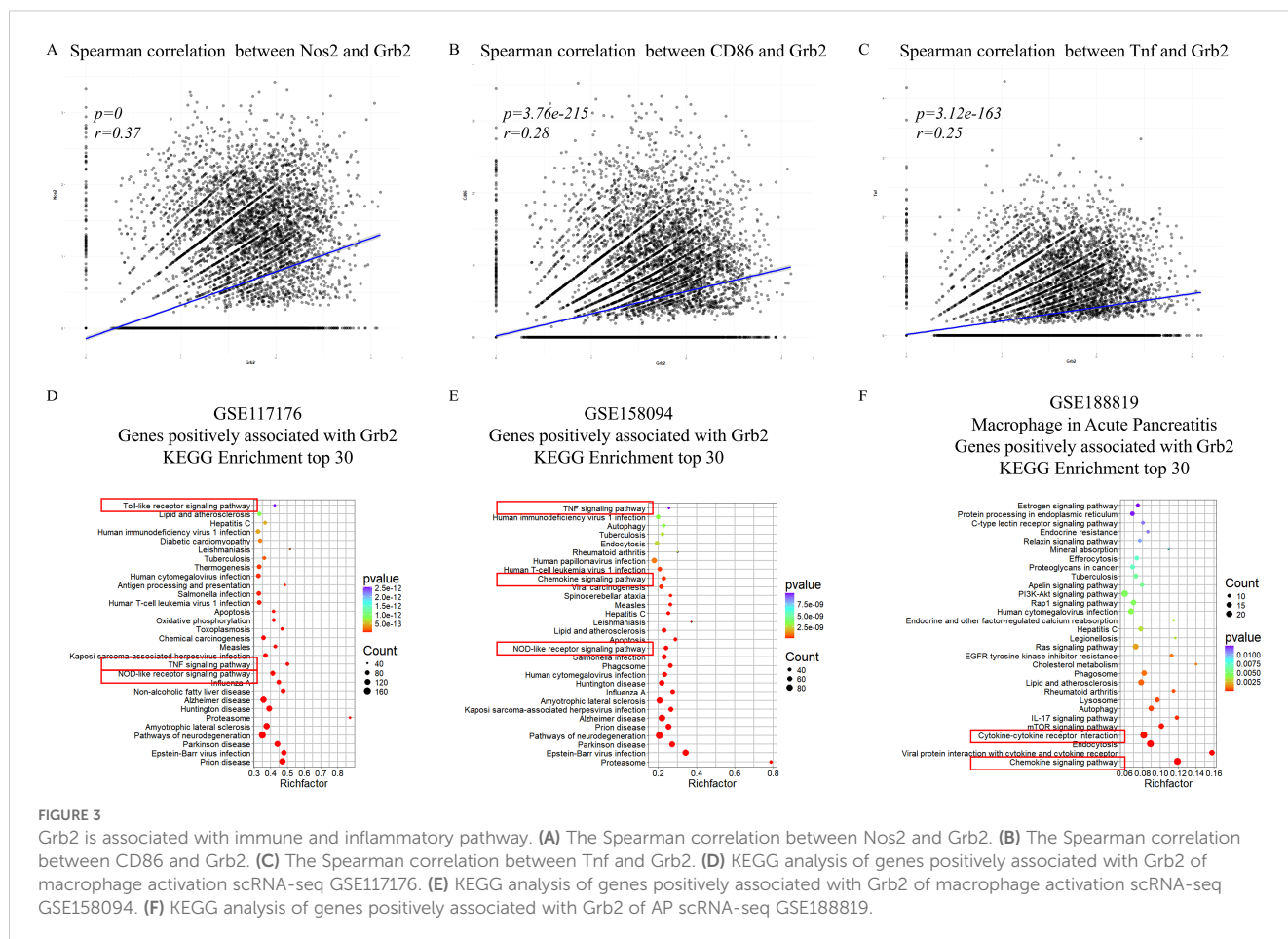
M2 macrophages (Figure 2C). Western blot results showed expression of Grb2 was up-regulated in M1 macrophages, but not in M2 macrophages. (Figures 2D, E). Thus, we hypothesized that Grb2 only exerts an effect on M1 macrophage activation.



Grb2 is associated with immune and inflammatory pathways

To verify the relationship between and macrophage activation. In GSE117176, correlation analysis revealed that Grb2 was positively correlated with M1 macrophage activation marker Nos2, CD86 and Tnf (Figures 3A–C), but not with M2 macrophage activation markers Chil3, Arg1, Retna and Mgl2 (Supplementary Figures S2A–D). Kyoto Encyclopedia of Genes

and Genomes (KEGG) analysis of genes positively related to Grb2 in the scRNA-seq data of M1 macrophage activation (GSE117176 and GSE158094) demonstrated that Grb2 was associated with immune and inflammatory pathways such as the NOD-like receptor signaling pathway and the TNF signaling pathway (Figures 3D, E). Additionally, in the scRNA-seq data of AP (GSE188819), Grb2 was also found to be related to immune and inflammatory pathways such as the Chemokine signaling pathway and the Cytokine-cytokine receptor interaction (Figure 3F).



Inhibition of Grb2 inhibits M1 macrophage activation

To clarify the role of Grb2 in macrophage activation, BMDMs were extracted to induce M1/M2 macrophage activation (Figure 4A). SiRNA was employed to silence the expression of Grb2 in BMDMs, and western blot was utilized to verify the silencing efficiency (Figure 4B). The silencing of Grb2 significantly inhibited M1 macrophage activation but had no significant impact on M2 activation (Figures 4C–F). Subsequently, the Grb2 inhibitor prexigebersen was used, and it was found that the results of the Grb2 inhibitor prexigebersen were consistent with those of Grb2 silencing (Figures 4G–J). All these results confirmed that Grb2 affected M1 macrophage activation and had little effect on M2.

Grb2 inhibitor alleviates AP *in vivo*

To explore the role of Grb2 *in vivo*, we established a classic acute pancreatitis model using caerulein and treat with the Grb2 inhibitor prexigebersen at 0h. In the Cae group, the pancreas of mice showed edema, inflammatory cell infiltration and cell necrosis. In the medium-dose prexigebersen treatment group, the edema, inflammatory cell infiltration and cell necrosis of pancreas of

mice were significantly improved (Figures 5A, B). Additionally, the levels of serum amylase and lipase levels in the medium-dose Prexigebersen group were lower than those in the Cae group (Figures 5C, D). We detected serum inflammatory factors Interleukin-6 (IL-6) and Monocyte Chemoattractant Protein-1 (MCP-1) in mice, reflecting inflammation in mice. IL-6 and MCP-1 were significantly increased in AP mice. Grb2 Inhibitor prexigebersen reduces serum IL-6 and MCP-1 levels (Figure 5D). We further verified in another PDL model, and the results showed that Grb2 inhibitor prexigebersen also alleviated the severity of PDL-induced acute pancreatitis (Supplementary Figures S3A–C). All these results indicate that the Grb2 inhibitor prexigebersen alleviates AP *in vivo*.

Grb2 inhibitor inhibits Nlrp3 and NF- κ B in macrophages

To further investigate the downstream mechanism of Grb2, we discovered that Nlrp3 and NF- κ B (Rela) were significantly up-regulated in the NOD-like receptor signaling pathway (Figure 6A). Recently, increasing evidence has suggested that Nlrp3 and NF- κ B play a crucial role in M1 macrophage activation (42–45). We observed that Nlrp3 and NF- κ B were upregulated during M1 macrophage activation *in vitro*. The Grb2 inhibitor prexigebersen

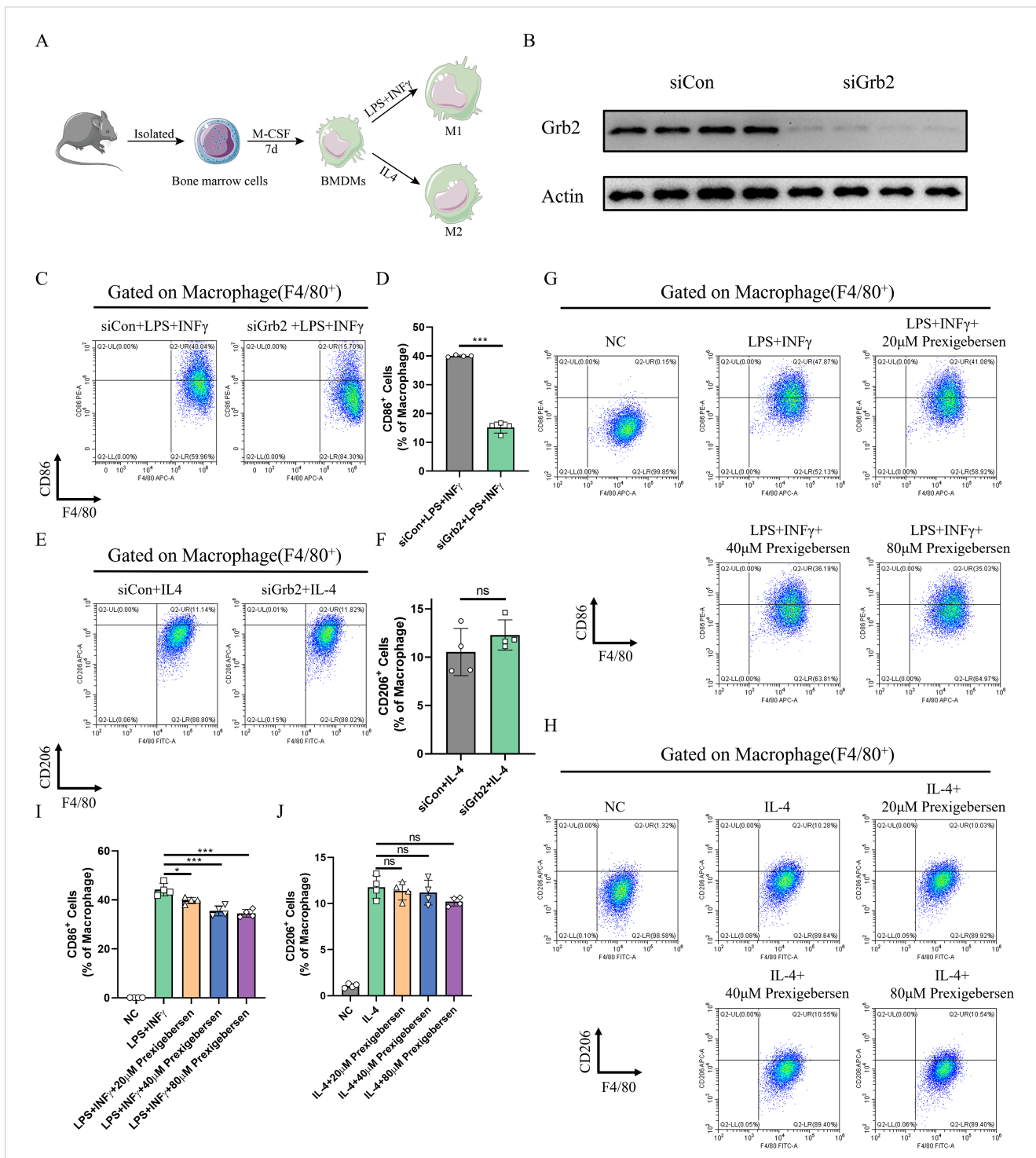
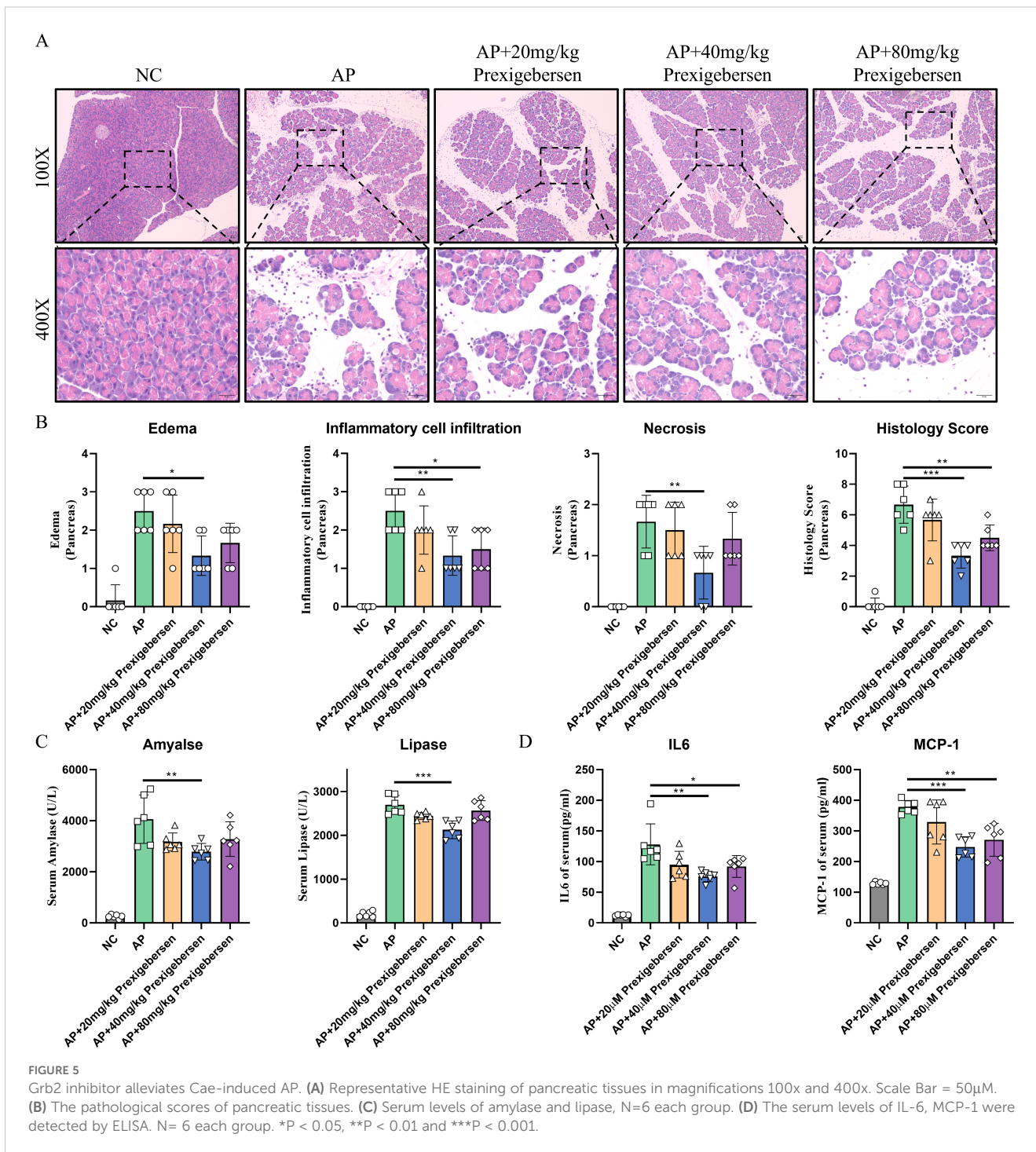


FIGURE 4

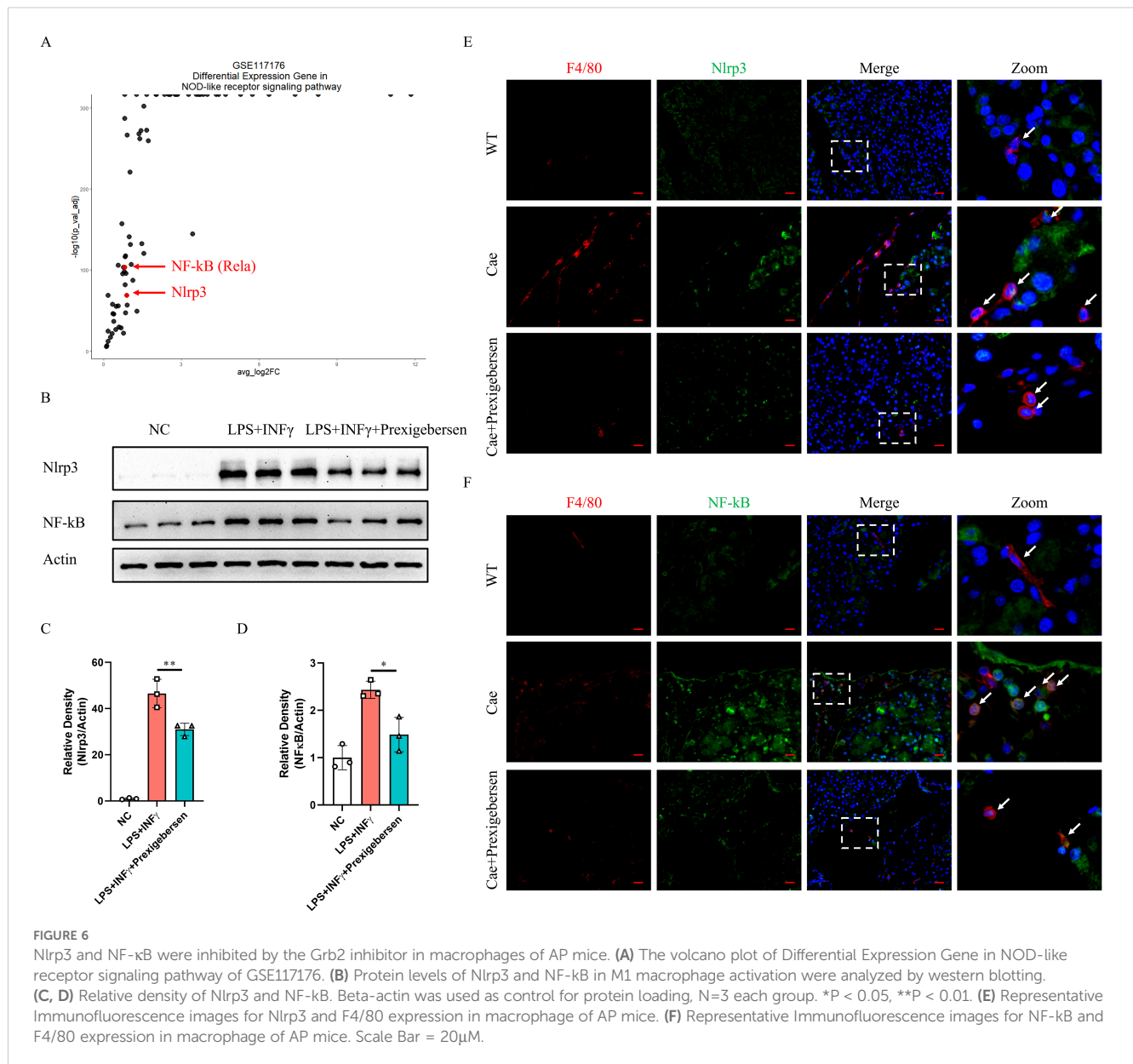
Inhibition of Grb2 inhibits M1 macrophage activation. (A) The flowchart of macrophage activation. (B) The silencing efficiency of Grb2 was analyzed by western blotting. (C, D) CD86 (M1 macrophage marker) and F4/80 (macrophage marker) expression levels in macrophages treated with Grb2 siRNA were detected by flow cytometry, N=4 each group. (E, F) CD206 (M2 macrophage marker) and F4/80 (macrophage marker) expression levels in macrophages treated with Grb2 siRNA were detected by flow cytometry, N=4 each group. (G) CD86 (M1 macrophage marker) and F4/80 (macrophage marker) expression levels in macrophages treated with Grb2 inhibitor prexigebersen were detected by flow cytometry, N=4 each group. (H) CD206 (M2 macrophage marker) and F4/80 (macrophage marker) expression levels in macrophages treated with Grb2 inhibitor prexigebersen were detected by flow cytometry, N=4 each group. (I, J) Quantification of M1/M2 macrophage activation detected by flow cytometry. *P < 0.05 and ***P < 0.001.



reversed the upregulation of Nlrp3 and NF-κB (Figures 6B–D). Consequently, we performed immunofluorescence analysis of pancreas of AP mice. The results demonstrated that Nlrp3 and NF-κB were up-regulated in macrophages during AP, and Grb2 inhibitor prexigebersen inhibited the expression of Nlrp3 and NF-κB in macrophage (Figures 6E, F). The above results indicate that Grb2 may influence M1 macrophage activation by regulating Nlrp3 and NF-κB.

Discussion

It is widely acknowledged that macrophages are one of essential cells during AP inflammation (9, 46–48). Through joint analysis of multiple RNA-seq and scRNA-seq databases, we discovered that Grb2 was highly expressed in macrophages during AP. Researchers have found that inhibition of Grb2 repolarized alveolar macrophages from M1 to M2 phenotype (49). Consequently, we



hypothesize that Grb2 may play a role in AP by regulating macrophage activation.

We discovered up-regulation of Grb2 in M1 macrophage activation through single-cell RNA-sequence analysis, whereas there was no significant alteration in M2. The result was validated by western blot. Subsequently, we further investigated the function of Grb2. Inhibition of Grb2 hindered M1 macrophage activation, but had no impact on M2. M1 macrophage activation affects AP. Inhibition of M1 macrophage activation can effectively mitigate AP (42, 50, 51). To study the effect of Grb2 in the pathological process of AP, we employed the Grb2 inhibitor prexigebersen to treat caerulein-induced AP mice and found that prexigebersen

alleviated the severity of AP and decreased the inflammatory response in AP mice.

A number of studies have demonstrated that Nlrp3 and NF-κB play a crucial role in M1 macrophage activation (52–55). We discovered that Nlrp3 and NF-κB were up-regulated in M1 macrophage activation. Both *in vitro* and *in vivo* experiments have proved that Nlrp3 and NF-κB were significantly up-regulated in M1 macrophage activation or macrophages of AP group, and Grb2 inhibitor prexigebersen inhibited the expression of Nlrp3 and NF-κB in macrophages. In summary, Inhibition of Grb2 can alleviate AP by down-regulating Nlrp3 and NF-κB of macrophage.

Conclusion

Overall, our study firstly demonstrates that inhibition of Grb2 can effectively prevent M1 macrophage activation and alleviate AP. Grb2 may potentially be an effective target of macrophage activation for the treatment of AP.

Data availability statement

The original contributions presented in the study are included in the article/**Supplementary Material**. Further inquiries can be directed to the corresponding authors.

Ethics statement

The animal study was approved by Laboratory Animal Ethics Committee of Yangzhou University. The study was conducted in accordance with the local legislation and institutional requirements.

Author contributions

QS: Validation, Visualization, Writing – original draft, Writing – review & editing. SW: Validation, Writing – original draft, Writing – review & editing. KW: Validation, Writing – original draft, Writing – review & editing. LW: Visualization, Writing – review & editing. WG: Supervision, Writing – review & editing. GL: Funding acquisition, Supervision, Writing – review & editing. WC: Funding acquisition, Supervision, Writing – review & editing. CY: Funding acquisition, Supervision, Writing – review & editing. BT: Supervision, Writing – review & editing. WL: Supervision, Writing – review & editing. YW: Conceptualization, Funding acquisition, Supervision, Writing – review & editing. WY: Conceptualization, Resources, Supervision, Writing – review & editing.

Funding

The author(s) declare that financial support was received for the research and/or publication of this article. This study was supported by the National Natural Science Foundation of China (No. 82270680, 82200721, 82300732); Jiangsu Funds for Distinguished Young Scholars (No. BK20240028); Policy guidance program (International science and technology cooperation) project of Yangzhou (No. YZ2023265); Yangzhou medical key disciplines incubation program (No. YZYXZDXK-11); Suzhou Key Laboratory of Digestive diseases of integrated Traditional Chinese and Western medicine (No. SZS2023001).

Acknowledgments

We are grateful to all the funds that have supported our research.

Conflict of interest

The authors declare that the research was conducted in the absence of any commercial or financial relationships that could be construed as a potential conflict of interest.

Generative AI statement

The author(s) declare that no Generative AI was used in the creation of this manuscript.

Publisher's note

All claims expressed in this article are solely those of the authors and do not necessarily represent those of their affiliated organizations, or those of the publisher, the editors and the reviewers. Any product that may be evaluated in this article, or claim that may be made by its manufacturer, is not guaranteed or endorsed by the publisher.

Supplementary material

The Supplementary Material for this article can be found online at: <https://www.frontiersin.org/articles/10.3389/fimmu.2025.1575880/full#supplementary-material>

SUPPLEMENTARY TABLE 1
Reagent table.

SUPPLEMENTARY TABLE 2
Antibody table

SUPPLEMENTARY TABLE 3
The list of genes for pathways of GSE65146

SUPPLEMENTARY TABLE 4
The list of genes for pathways of GSE109227

SUPPLEMENTARY TABLE 5
The list of genes for cluster of STEM clustering analysis

SUPPLEMENTARY TABLE 6
Markers for identifying cell types.

SUPPLEMENTARY FIGURE 1
GRB2 is upregulated in PBMC of AP patients. **(A)** Protein levels of GRB2 in PBMC were analyzed by western blotting. **(B)** Relative density of Grb2. Beta-actin was used as control for protein loading, N=4 each group. *P < 0.05.

SUPPLEMENTARY FIGURE 2
Grb2 is not associated with M2 marker. **(A)** The Spearman correlation between Chil3 and Grb2. **(B)** The Spearman correlation between Arg1 and Grb2. **(C)** The Spearman correlation between Retnla and Grb2. **(D)** The Spearman correlation between Mgl2 and Grb2.

SUPPLEMENTARY FIGURE 3
Grb2 inhibitor alleviates PDL-induced AP. **(A)** Representative HE staining of pancreatic tissues in magnifications 100x and 400x. Scale Bar = 50μM. **(B)** Serum levels of amylase and lipase. **(C)** The pathological scores of pancreatic tissues. N=6 each group. N= 6 each group. *P < 0.05, **P < 0.01.

References

1. Trikudanathan G, Yazici C, Evans Phillips A, Forsmark CE. Diagnosis and management of acute pancreatitis. *Gastroenterology*. (2024) 167:673–88. doi: 10.1053/j.gastro.2024.02.052
2. Zhou Y, Huang X, Jin Y, Qiu M, Ambe PC, Basharat Z, et al. The role of mitochondrial damage-associated molecular patterns in acute pancreatitis. *BioMed Pharmacother*. (2024) 175:116690. doi: 10.1016/j.biopha.2024.116690
3. Aney KJ, Jeong WJ, Vallejo AF, Burdziak C, Chen E, Wang A, et al. Novel approach for pancreas transcriptomics reveals the cellular landscape in homeostasis and acute pancreatitis. *Gastroenterology*. (2024) 166(6):1100–13. doi: 10.1053/j.gastro.2024.01.043
4. Fang Z, Li J, Cao F, Li F. Integration of scRNA-seq and bulk RNA-seq reveals molecular characterization of the immune microenvironment in acute pancreatitis. *Biomolecules*. (2022) 13:78. doi: 10.3390/biom13010078
5. Zhu Q, Yuan C, Wang D, Tu B, Chen W, Dong X, et al. The TRIM28/miR133a/CD47 axis acts as a potential therapeutic target in pancreatic necrosis by impairing efferocytosis. *Mol Ther*. (2024) 32(9):3025–41. doi: 10.1016/j.yymthe.2024.06.005
6. Manohar M, Jones EK, Rubin SJS, Subrahmanyam PB, Swaminathan G, Mikhail D, et al. Novel circulating and tissue monocytes as well as macrophages in pancreatitis and recovery. *Gastroenterology*. (2021) 161(6):2014–2029.e14. doi: 10.1053/j.gastro.2021.08.033
7. Han F, Ding ZF, Shi XL, Zhu QT, Shen QH, Xu XM, et al. Irisin inhibits neutrophil extracellular traps formation and protects against acute pancreatitis in mice. *Redox Biol*. (2023) 64:102787. doi: 10.1016/j.redox.2023.102787
8. Li G, Liu L, Lu T, Sui Y, Zhang C, Wang Y, et al. Gut microbiota aggravates neutrophil extracellular traps-induced pancreatic injury in hypertriglyceridemic pancreatitis. *Nat Commun*. (2023) 14(1):6179. doi: 10.1038/s41467-023-41950-y
9. Wu J, Zhang L, Shi J, He R, Yang W, Habtezion A, et al. Macrophage phenotypic switch orchestrates the inflammation and repair/regeneration following acute pancreatitis injury. *EBioMedicine*. (2020) 58:102920. doi: 10.1016/j.ebiom.2020.102920
10. Yang J, Tang X, Li B, Shi J. Sphingosine 1-phosphate receptor 2 mediated early stages of pancreatic and systemic inflammatory responses via NF-kappa B activation in acute pancreatitis. *Cell Commun Signal*. (2022) 20:157. doi: 10.1186/s12964-022-00971-8
11. Wang D, Liu G, Meng Y, Chen H, Ye Z, Jing J. The configuration of GRB2 in protein interaction and signal transduction. *Biomolecules*. (2024) 14:259. doi: 10.3390/biom14030259
12. Dias RVR, Pedro RP, Sanches MN, Moreira GC, Leite VBP, Caruso IP, et al. Unveiling metastable ensembles of GRB2 and the relevance of interdomain communication during folding. *J Chem Inf Model*. (2023) 63(20):6344–53. doi: 10.1021/acs.jcim.3c00955
13. Zhou J, Tu D, Peng R, Tang Y, Deng Q, Su B, et al. RNF173 suppresses RAF/MEK/ERK signaling to regulate invasion and metastasis via GRB2 ubiquitination in Hepatocellular Carcinoma. *Cell Commun Signal*. (2023) 21(1):224. doi: 10.1186/s12964-023-01241-x
14. Lv J, Zhang S, Wu H, Lu J, Lu Y, Wang F, et al. Deubiquitinase PSMD14 enhances hepatocellular carcinoma growth and metastasis by stabilizing GRB2. *Cancer Lett*. (2020) 469:22–34. doi: 10.1016/j.canlet.2019.10.025
15. Wang LN, Zhang ZT, Wang L, Wei HX, Zhang T. TGF- β 1/SH2B3 axis regulates anoikis resistance and EMT of lung cancer cells by modulating JAK2/STAT3 and SHP2/Grb2 signaling pathways. *Cell Death Dis*. (2022) 13(5):472. doi: 10.1038/s41419-022-04890-x
16. Hou B, Huang H, Li Y, Liang J, Xi Z, Jiang X, et al. Grb2 interacts with necrosome components and is involved in rasfonin-induced necroptosis. *Cell Death Discovery*. (2022) 8(1):319. doi: 10.1038/s41420-022-01106-1
17. Montero-Vergara J, Plachetta K, Kinch L, Bernhardt S, Kashyap K, Levine B, et al. GRB2 is a BECN1 interacting protein that regulates autophagy. *Cell Death Dis*. (2024) 15(1):14. doi: 10.1038/s41419-023-06387-7
18. Zhao H, Mao H. ERRF1 exacerbates hepatic ischemia reperfusion injury by promoting hepatocyte apoptosis and ferroptosis in a GRB2-dependent manner. *Mol Med*. (2024) 30:82. doi: 10.1186/s10020-024-00837-4
19. Chen Y, Wu J, Yan H, Cheng Y, Wang Y, Yang Y, et al. Lymecycline reverses acquired EGFR-TKI resistance in non-small-cell lung cancer by targeting GRB2. *Pharmacol Res*. (2020) 159:105007. doi: 10.1016/j.phrs.2020.105007
20. Choi S, Hatzihristidis T, Gaud G, Dutta A, Lee J, Arya A, et al. GRB2 promotes thymocyte positive selection by facilitating THEMIS-mediated inactivation of SHP1. *J Exp Med*. (2023) 220(7):e20221649. doi: 10.1084/jem.20221649
21. Zhao X, Cui P, Hu G, Wang C, Jiang L, Zhao J, et al. PIP5k1 β controls bone homeostasis through modulating both osteoclast and osteoblast differentiation. *J Mol Cell Biol*. (2020) 12(11):55–70. doi: 10.1093/jmcb/mjz028
22. Benamar M, Harb H, Chen Q, Wang M, Chan TMF, Fong J, et al. A common IL-4 receptor variant promotes asthma severity via a T(reg) cell GRB2-IL-6-Notch4 circuit. *Allergy*. (2022) 77:3377–87. doi: 10.1111/all.15444
23. Diwan BA, Ramakrishna G, Anderson LM, Ramljak D. Overexpression of Grb2 in inflammatory lesions and preneoplastic foci and tumors induced by N-nitrosodimethylamine in Helicobacter hepaticus-infected and -noninfected A/J mice. *Toxicol Pathol*. (2000) 28:548–54. doi: 10.1177/019262330002800407
24. Li J, Chang W, Li J, Zhao X, Li X. IL-22-mediated microRNA-124-3p/GRB2 axis regulates hyperproliferation and inflammatory response of keratinocytes in psoriasis. *Arch Dermatol Res*. (2025) 317:227. doi: 10.1007/s00403-024-03668-9
25. Liu X, Zhu Q, Zhang M, Yin T, Xu R, Xiao W, et al. Isoliquiritigenin ameliorates acute pancreatitis in mice via inhibition of oxidative stress and modulation of the nrf2/HO-1 pathway. *Oxid Med Cell Longev*. (2018) 2018:7161592. doi: 10.1155/2018/7161592
26. Norberg KJ, Nania S, Li X, Gao H, Sztatny P, Segersvärd R, et al. RCAN1 is a marker of oxidative stress, induced in acute pancreatitis. *Pancreatology*. (2018) 18(7):734–41. doi: 10.1016/j.pan.2018.08.005
27. Ritchie ME, Phipson B, Wu D, Hu Y, Law CW, Shi W, et al. limma powers differential expression analyses for RNA-seq and microarray studies. *Nucleic Acids Res*. (2015) 43(7):e47. doi: 10.1093/nar/gkv007
28. Wu T, Hu E, Xu S, Chen M, Guo P, Dai Z, et al. clusterProfiler 4.0: A universal enrichment tool for interpreting omics data. *Innovation (Camb)*. (2021) 2(3):100141. doi: 10.1016/j.xinn.2021.100141
29. Yu G, Wang LG, Han Y, He QY. clusterProfiler: an R package for comparing biological themes among gene clusters. *OMICS*. (2012) 16:284–7. doi: 10.1089/omi.2011.0118
30. Mishra AK, Rodriguez M, Torres AY, Smith M, Rodriguez A, Bond A, Morrissey MA, et al. Hyperactive Rac stimulates cannibalism of living target cells and enhances CAR-M-mediated cancer cell killing. *Proc Natl Acad Sci U S A*. (2023) 120(52):e2310221120. doi: 10.1073/pnas.2310221120
31. Love MI, Huber W, Anders S. Moderated estimation of fold change and dispersion for RNA-seq data with DESeq2. *Genome Biol*. (2014) 15:550. doi: 10.1186/s13059-014-0550-8
32. Chen Y, Lun AT, Smyth GK. From reads to genes to pathways: differential expression analysis of RNA-Seq experiments using Rsubread and the edgeR quasi-likelihood pipeline. *F1000Res*. (2016) 5:1438. doi: 10.12688/f1000research.8987.2
33. McCarthy DJ, Chen Y, Smyth GK. Differential expression analysis of multifactor RNA-Seq experiments with respect to biological variation. *Nucleic Acids Res*. (2012) 40:4288–97. doi: 10.1093/nar/gks042
34. Robinson MD, McCarthy DJ, Smyth GK. edgeR: a Bioconductor package for differential expression analysis of digital gene expression data. *Bioinformatics*. (2010) 26:139–40. doi: 10.1093/bioinformatics/btp616
35. Melendez E, Chondronasiou D, Mosteiro L, Martínez de Villarreal J, Fernández-Alfara M, Lynch CJ, et al. Natural killer cells act as an extrinsic barrier for *in vivo* reprogramming. *Development*. (2022) 149(8):dev200361. doi: 10.1242/dev.200361
36. Li C, Menoret A, Farragher C, Ouyang Z, Bonin C, Holvoet P, et al. Single cell transcriptomics based-MacSpectrum reveals novel macrophage activation signatures in diseases. *JCI Insight*. (2019) 5(10):e126453. doi: 10.1172/jci.insight.126453
37. Liu SX, Gustafson HH, Jackson DL, Pun SH, Trapnell C. Trajectory analysis quantifies transcriptional plasticity during macrophage polarization. *Sci Rep*. (2020) 10:12273. doi: 10.1038/s41598-020-68766-w
38. Hao Y, Stuart T, Kowalski MH, Choudhary S, Hoffman P, Hartman A, et al. Dictionary learning for integrative, multimodal and scalable single-cell analysis. *Nat Biotechnol*. (2024) 42(2):293–304. doi: 10.1038/s41587-023-01767-y
39. Korsunsky I, Millard N, Fan J, Slowikowski K, Zhang F, Wei K, et al. Fast, sensitive and accurate integration of single-cell data with Harmony. *Nat Methods*. (2019) 16(12):1289–96. doi: 10.1038/s41592-019-0619-0
40. Ernst J, Nau GJ, Bar-Joseph Z. Clustering short time series gene expression data. *Bioinformatics*. (2005) 21 Suppl 1:i159–68. doi: 10.1093/bioinformatics/bti1022
41. Ernst J, Bar-Joseph Z. STEM: a tool for the analysis of short time series gene expression data. *BMC Bioinf*. (2006) 7:191. doi: 10.1186/1471-2105-7-191
42. Han X, Ni J, Wu Z, Wu J, Li B, Ye X, et al. Myeloid-specific dopamine D(2) receptor signalling controls inflammation in acute pancreatitis via inhibiting M1 macrophage. *Br J Pharmacol*. (2020) 177(13):2991–3008. doi: 10.1111/bph.v177.13
43. He R, Li Y, Han C, Lin R, Qian W, Hou X. L-Fucose ameliorates DSS-induced acute colitis via inhibiting macrophage M1 polarization and inhibiting NLRP3 inflammasome and NF-kB activation. *Int Immunopharmacol*. (2019) 73:379–88. doi: 10.1016/j.intimp.2019.05.013
44. Fang C, Zhong R, Lu S, Yu G, Liu Z, Yan C, et al. TREM2 promotes macrophage polarization from M1 to M2 and suppresses osteoarthritis through the NF-kB/CXCL3 axis. *Int J Biol Sci*. (2024) 20(6):1992–2007. doi: 10.7150/ijbs.91519
45. Zhang S, Hou B, Xu A, Wen Y, Zhu X, Cai W, et al. Ganlu formula ethyl acetate extract (GLEE) blocked the development of experimental arthritis by inhibiting NLRP3 activation and reducing M1 type macrophage polarization. *J Ethnopharmacol*. (2024) 332:118377. doi: 10.1016/j.jep.2024.118377
46. Zhang L, Shi J, Du D, Niu N, Liu S, Yang X, et al. Ketogenesis acts as an endogenous protective programme to restrain inflammatory macrophage activation during acute pancreatitis. *EBioMedicine*. (2022) 78:103959. doi: 10.1016/j.ebiom.2022.103959

47. Peng C, Tu G, Wang J, Wang Y, Wu P, Yu L, et al. MLKL signaling regulates macrophage polarization in acute pancreatitis through CXCL10. *Cell Death Dis.* (2023) 14(2):155. doi: 10.1038/s41419-023-05655-w
48. Wang LJ, Jin YL, Pei WL, Li JC, Zhang RL, Wang JJ, et al. Amuc₁₁₀₀ pretreatment alleviates acute pancreatitis in a mouse model through regulating gut microbiota and inhibiting inflammatory infiltration. *Acta Pharmacol Sin.* (2024) 45(3):570–80. doi: 10.1038/s41401-023-01186-4
49. Wang Q, Hong L, Chen M, Shi J, Lin X, Huang L, et al. Targeting M2 Macrophages Alleviates Airway Inflammation and Remodeling in Asthmatic Mice via miR-378a-3p/GRB2 Pathway. *Front Mol Biosci.* (2021) 8:717969. doi: 10.3389/fmolb.2021.717969
50. Tang DS, Cao F, Yan CS, Cui JT, Guo XY, Cheng L, et al. Acinar cell-derived extracellular vesicle miRNA-183-5p aggravates acute pancreatitis by promoting M1 macrophage polarization through downregulation of foxO1. *Front Immunol.* (2022) 13:869207. doi: 10.3389/fimmu.2022.869207
51. Song H, Zhang J, Lou N, Jiang X, Cui Y, Liu J, et al. Emodin nanocapsules inhibit acute pancreatitis by regulating lipid metabolic reprogramming in macrophage polarization. *Phytomedicine.* (2024) 130:155763. doi: 10.1016/j.phymed.2024.155763
52. Sun J, Zeng Q, Wu Z, Huang L, Sun T, Ling C, et al. Berberine inhibits NLRP3 inflammasome activation and proinflammatory macrophage M1 polarization to accelerate peripheral nerve regeneration. *Neurotherapeutics.* (2024) 21(4):e00347. doi: 10.1016/j.neurot.2024.e00347
53. Zhao YX, Sun YY, Li LY, Li XF, Li HD, Chen X, et al. Rab11b promotes M1-like macrophage polarization by restraining autophagic degradation of NLRP3 in alcohol-associated liver disease. *Acta Pharmacol Sin.* (2024) 46(1):134–46. doi: 10.1038/s41401-024-01333-5
54. Yang S, Yin Y, Sun Y, Ai D, Xia X, Xu X, et al. AZGP1 aggravates macrophage M1 polarization and pyroptosis in periodontitis. *J Dent Res.* (2024) 103(6):631–41. doi: 10.1177/00220345241235616
55. Ma Y, Liu Y, Zhong Y, Li X, Xu Y, Chen L, et al. Oroxylin A attenuates psoriasiform skin inflammation by direct targeting p62 (sequestosome 1) via suppressing M1 macrophage polarization. *Br J Pharmacol.* (2024) 181(24):5110–32. doi: 10.1111/bph.v181.24